Biochimica et Biophysica Acta 1808 (2011) 2059–2066

Contents lists available at ScienceDirect

Biochimica et Biophysica Acta

journal homepage: www.elsevier.com/locate/bbamem

Expression of a chloroplast ATP/ADP transporter in *E. coli* membranes: Behind the Mistic strategy

Aurélien Deniaud [a,b,c,1], Florent Bernaudat [a,b,c], Annie Frelet-Barrand [d,e,f,g,2], Céline Juillan-Binard [a,b,c], Thierry Vernet [a,b,c], Norbert Rolland [d,e,f,g], Eva Pebay-Peyroula [a,b,c,*]

[a] CEA, Institut de Biologie Structurale Jean-Pierre Ebel, 41 rue Jules Horowitz, F-38027 Grenoble, France
[b] CNRS, Institut de Biologie Structurale Jean-Pierre Ebel, F-38027 Grenoble, France
[c] Université Joseph Fourier Grenoble 1, Institut de Biologie Structurale Jean-Pierre Ebel, F-38027 Grenoble, France
[d] CNRS, Laboratoire de Physiologie Cellulaire Végétale, UMR5168, F-38000 Grenoble, France
[e] CEA, LPCV, Institut de Recherches en Technologies et Sciences pour le Vivant, F-38000 Grenoble, France
[f] Université Joseph Fourier Grenoble 1, LPCV, F-38000 Grenoble, France
[g] INRA, LPCV, UMR1200, F-38000 Grenoble, France

ARTICLE INFO

Article history:
Received 18 February 2011
Received in revised form 11 April 2011
Accepted 15 April 2011
Available online 30 April 2011

Keywords:
Membrane protein heterologous expression
Mistic fusion strategy
ATP/ADP chloroplast transporter
In vivo fusion cleavage

ABSTRACT

Eukaryotic membrane protein expression is still a major bottleneck for structural studies. Production in *E. coli* often leads to low expression level and/or aggregated proteins. In the last decade, strategies relying on new fusion protein expression revealed promising results. Fusion with the amphipatic Mistic protein has been described to favor expression in *E. coli* membranes. Although, this approach has already been reported for a few membrane proteins, little is known about the activity of the fused proteins. We used this strategy and obtained high expression levels of a chloroplast ATP/ADP transporter from *A. thaliana* (NTT1) and characterized its transport properties. NTT1 fused to Mistic has a very low transport activity which can be recovered after *in vivo* Mistic fusion cleavage. Moreover, detailed molecular characterization of purified NTT1 mature form, NTT1 fused to Mistic or NTT1 cleaved-off from this fusion highlights the correct fold of the latter one. Therefore, considering the higher quantity of purified NTT1 mature form obtained *via* the Mistic fusion approach, this is a valuable strategy for obtaining quantities of pure and active proteins that are adequate for structural studies.

1. Introduction

Although 20 to 30% of the genomes code for membrane proteins [1], the latter represent less than 1% of the structures deposited in the PDB [2]. Membrane proteins control all the signaling and exchanges between cells and intracellular compartments and are therefore key elements in most biological processes. Indeed, 60 to 70% of drugs target membrane proteins. The discrepancy between their relevance and the lack of structural information lies in the difficulties to handle such amphipatic molecules. It is well known that their overexpression into the membrane of host cells is often highly poisonous. Solubilization of the produced proteins in a stable and functional conformation is a second major bottleneck. This process requires exploring various amphiphiles, including lipids, and characterizing the protein-detergent complex using a combination of complementary biochemical and biophysical techniques, none of them being sufficient on its own. Finally, crystallization still remains a difficult step although novel methods based on lipidic phases and developed over the last 15 years have opened new ways of investigations [3–5]. The success rate of crystallization strongly relates to the quality of the previous steps: protein expression and solubilization. Because of the importance of membrane proteins, several teams have in the last decade extensively explored various expression systems [6,7]. Therefore, the best strategy to crystallize a new protein remains to explore these methods in parallel.

In a recent medium-scale approach aiming to overexpress membrane proteins, 17 different intrinsic membrane proteins have been tested for expression in six expression systems. Among those, the recently described Mistic fusion approach has been successfully tested. Indeed, for any of the 12 membrane proteins effectively expressed in *E. coli*, the Mistic fusion has always led to increased expression levels. Furthermore, in some cases Mistic fusion delivered protein amounts compatible with structural studies. However, the number of publications related to this Mistic fusion approach and describing integral membrane protein overexpression remains low [8–13] and the membrane integration mechanism of Mistic is still elusive. Previous publications mainly report about expression levels and some biochemical or biophysical

* Corresponding author at: Institut de Biologie Structurale, 41 Rue Jules Horowitz, 38027 Grenoble Cedex 1, France. Tel.: +33 4 38 78 34 82/95 83; fax: +33 4 38 78 94 84.
E-mail address: eva.pebay-peyroula@ibs.fr (E. Pebay-Peyroula).
[1] Present address: European Molecular Biology Laboratory, Grenoble Outstation, F-38000 Grenoble, France.
[2] Present address: CEA, iBiTec-S, Service de Bioénergétique Biologie Structurale et Mécanismes, CNRS URA 2096, Laboratoire Stress Oxydant et Détoxification, F-91191 Gif sur Yvette, France.

0005-2736/$ – see front matter © 2011 Elsevier B.V. All rights reserved.
doi:10.1016/j.bbamem.2011.04.011

characterizations but only a few of them describe functional properties of the overexpressed proteins [10,13]. So far no functional validation has been performed for a membrane transporter fused to Mistic. Bacteriorhodopsin is the only membrane protein with several trans-membrane helices for which functional assays have been reported [10].

The present study focuses on the chloroplast ATP/ADP transporter from *Arabidopsis thaliana* (NTT1) [14,15], one of the 17 membrane proteins previously studied. NTT1 is a 60 kDa transporter located in the inner membrane of the chloroplast envelope that exchanges ATP with ADP [14,16]. Eleven to twelve trans-membrane helices are predicted from its primary sequence. As most chloroplast proteins, the NTT1 N-terminus (chloroplast targeting sequence) is cleaved-off during its integration into the chloroplast envelope membrane. After cleavage, the mature form of the protein is folded and turns into a functional transporter [14,15]. In the late nineties, it has been shown that it was possible to express this transporter in a functional form in *E. coli* membranes [14]. Further functional characterization led to the discovery of charged residues crucial for steady-state ATP/ADP exchange [17]. More recently, studies have focused on bacterial homologues of NTT1 [16,18] providing a general model for transport of both bacterial and plastidial ATP/ADP transporters. It has thus been proposed that these proteins transport ADP + Pi against ATP in a counter-exchange way [16]. These recent reports provided the first purification procedure of NTT1s expressed in bacteria [16,18]. Our medium-scale overexpression approach confirmed that *A. thaliana* NTT1 can be well expressed in *E. coli* but also indicated that, when fused to Mistic, NTT1 can be expressed at higher level. We previously reported that NTT1 is expressed as an active transporter in *L. lactis* but at a lower yield [19]. We herein further explored the production of NTT1 in *E. coli* and compared the activity of both proteins, the mature form of NTT1 and NTT1 bearing a N-terminal Mistic fusion (misNTT1). Differences in functional properties are evidenced. They are characterized and discussed in light of different constructs and biochemical and biophysical approaches.

2. Material and methods

2.1. Materials

Detergents were obtained from Anatrace, all other chemicals from Sigma.

2.2. Molecular cloning and DNA manipulation

The different constructs used are depicted in Fig. S1 and the primers used for their generation are listed in the Table S1. NTT1 UniProt sequence number Q39002 lacking the first 79 residues composing the N-terminal leader peptide has been used for further cloning. NTT1 has been cloned by the Gateway technology (Invitrogen) into pDEST17 (Invitrogen) and misNTT1 into pDEST-Mistic. Thus, schematically the NTT1 expressed sequence is MSYY-HHHHHH-LE-*AttB1site -NTT1seq-Streptag* and the misNTT1 expressed sequence is MSYY-HHHHHH-LE-*Mistic*-LE-*AttB1site-NTT1seq-Streptag*. Amino acid sequences of all linkers are described in Table S1. misTmNTT1 has also been cloned by the Gateway technology using a modified pDEST-Mistic vector containing an insert between the ORF of Mistic and the *Att*B1 site. This insert yields an additional transmembrane domain sequence in the misTm construct (see Table S1). The longer linker in mislinkNTT1 and the TEV and the factor Xa cleavage sites have been introduced in the misNTT1 construct using the Quick Change Site Directed Mutagenesis kit from Agilent Technologies with the primers mislinkNTT1for, mislinkNTT1rev, misTevNTT1for, misTevNTT1rev, misXaNTT1for and misXaNTT1rev (Table S1). The linker of mislink sequence is described in the Table S1. The tetracycline-inducible TEV plasmid has been generated in a two-step PCR [20]. The first PCR was done with Pfu polymerase (New England Biolabs) to amplify MBP-TEV coding cDNA using the primers pTEVfor and pTEVrev. The purified PCR product was then used as primers in a Quick Change PCR (Agilent) with pG-KJE6 as matrix in order to insert MBP-TEV into the pG-KJE6 [21].

2.3. Expression and purification

The different constructs were expressed in C43(DE3) cells [22]. Freshly transformed cells were grown in TB medium at 37 °C until $OD_{600nm} = 0.6$ was reached. Then, protein overexpression was induced by addition of 0.5 mM IPTG and overnight growth at 20 °C. For the expression of the in-membrane cleaved form of misTevNTT1, the protein was always expressed overnight. The TEV protease (TEV) was induced by the addition of 20 ng/mL tetracycline either at the same time as misTevNTT1 or after the overnight expression to have a sequential expression, misTevNTT1 then TEV. In the latter case, TEV was expressed for 3 h. All bacterial cultures were stopped after this 3 h TEV induction. Overexpressed proteins have been quantified by *Strep*-Tactin peroxidase (IBA) or anti-histag peroxidase (Sigma) western-blots with standard proteins.

For membrane preparation, cell pellets were resuspended in 100 mM Tris pH 8, 500 mM NaCl, 1 mM $MgCl_2$, DNAse and complete protease inhibitors 1 pill/50 mL (Roche). Cells were disrupted by two passages through a microfluidizer cell at 180 psi (Microfluidics). Unbroken cells were removed by centrifugation at 10,000 × *g* for 15 min and then membranes were sedimented at 150,000 × *g* for 90 min. Finally, these membranes were resuspended at 20 mg/mL in 100 mM Tris pH 8, 500 mM NaCl and stored at −80 °C.

For protein purification, membranes were solubilized in 50 mM Tris pH 8, 100 mM NaCl, 1% (w:v) LAPAO, 10 mM imidazole, EDTA-free complete protease inhibitors 1 pill/50 mL (Roche) for 1 h at 4 °C with constant mixing. Unsolubilized membranes were removed by centrifugation at 100,000 × *g* for 1 h at 4 °C. Then the supernatant was incubated with Ni-NTA beads (Qiagen) for 2 h at 4 °C with constant stirring. The resin was then washed with 20 mM Tris pH 8, 100 mM NaCl, 0.1% (w:v) LAPAO containing 10 mM imidazole in a first wash and 20 mM imidazole in a second wash. Proteins were eluted from Ni-NTA beads using the same buffer containing 200 mM imidazole. Buffer was exchanged using a PD10 column (GE-healthcare) to 20 mM Tris pH 8, 100 mM NaCl, 0.1% (w:v) LAPAO, just before mixing with *Strep*-Tactin beads (IBA). The mixture was incubated overnight with constant stirring at 4 °C. The beads were extensively washed with the PD10 buffer and the final elution was performed in the same buffer containing 3 mM desthiobiotin (IBA). Further buffer exchange was performed using a PD10 column in order to remove desthiobiotin. For clmisXaNTT1 purification, the fusion was cleaved between the Ni-NTA and the *Strep*-Tactin chromatography steps by an overnight incubation of the Ni-NTA eluted proteins with factor Xa using 1 unit of protease for 50 μg of proteins. When required, the purified proteins were concentrated on an Amicon concentrator with a 50 kDa cut-off. Size exclusion chromatography (SEC) experiments were performed on a 20 mL analytical superdex-200 in 20 mM Tris pH 8, 100 mM NaCl, 0.1% (w:v) LAPAO at a 0.4 mL/min flow rate.

2.4. Activity measurements

Activities were measured on whole *E. coli* cells in conditions similar to those described in [23,24]. Briefly, after protein overexpression, cells were washed and resuspended in 50 mM phosphate buffer pH 7.5. For radioactivity experiments, 30 μL of cells at 100 μg/μL were incubated with radioactive ATP (3000 mCi/mmol, Perkin Elmer) at 25 °C for indicated time periods. ATP uptake was quenched by addition of 1 mL ice-cold phosphate buffer, subsequently filtered through a 0.45 μm filter (Millipore) and washed three times with 1 mL of phosphate buffer. The radioactivity retained on the filters was quantified in 3.5 mL of water in a Multi-Purpose Scintillation Counter (Beckman Coulter, Fullerton, USA). For luminescence experiments

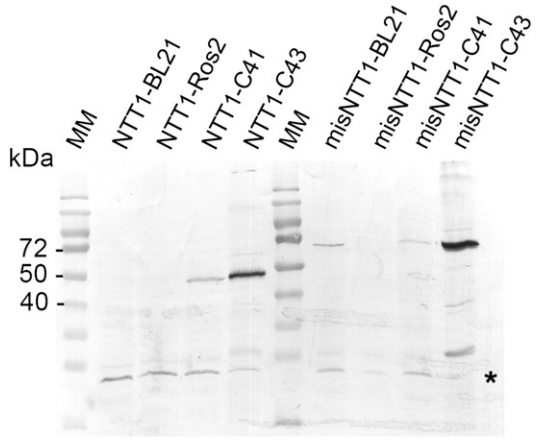

Fig. 1. NTT1 and misNTT1 expressions in various *E. coli* strains. NTT1 and misNTT1 total expression after overnight induction in different strains: BL21(DE3), Rosetta2(DE3) (Ros2), C41(DE3), C43(DE3). Overexpressed proteins were detected by *Strep*-Tactin peroxidase western-blots. NTT1 is observed around the 50 kDa marker and misNTT1 around the 72 kDa marker. For NTT1 1 mg of bacteria have been loaded per lane and for misNTT1 500 µg. * indicates the biotin carboxyl carrier protein (BCCP), an endogenously biotinylated protein always detected by *Strep*-Tactin peroxidase in whole bacterial extracts. MM corresponds to the molecular weight marker lanes.

200 µL of cells were diluted in 1 mL of 50 mM phosphate buffer pH 7.5 containing 40 µM luciferin (Sigma) and 40 µg/mL luciferase (Sigma) in a 1-mL cuvette and the luminescence was monitored. When the baseline is stable, the desired ADP concentration is added to the cuvette and the luminescence is monitored during 5 min. For all activity experiments, whole cell proteins were separated by SDS-PAGE and transferred onto nitrocellulose membrane. The different NTT1 constructs were then detected with anti-Histag peroxidase or *Strep*-Tactin peroxidase conjugates, depending on the construct used. Western-blots were revealed on a Kodak 4000MM image station and quantification was done with the Molecular Imaging Software (Kodak) using different concentrations of pure NTT1 and misNTT1 as standards. V_M and K_M determinations have been performed with the software KaleidaGraph by using Michaelis–Menten equation to fit the experimental data.

2.5. Limited proteolysis

Limited proteolysis experiments were performed on pure proteins in LAPAO as previously described in [25].

2.6. Analytical centrifugation

The experiments were performed using a Beckman XL-I analytical ultracentrifuge and an An-60Ti rotor (Beckman Coulter) in 12 mm or 3 mm optical path length cell equipped with sapphire windows. Sample density and viscosity were 1.004 g/mL and 1.32 mPa.s, respectively. 280 nm absorbance profiles were measured during 16 h at 42,000 rpm and 10 °C. Analysis was done in terms of continuous size-distribution (c(s)) with the Sedfit program [26], considering 200 particles with sedimentation coefficients, s, between 0.1 and 20 S, with a frictional ratio of 1.25 and a partial specific volume of 0.89 mL/g, and applying regularization procedure with a confidence level of 0.68.

3. Results and discussion

3.1. Mistic fusion enhances the expression level but alters NTT1 activity

3.1.1. Protein expression

The different constructs used in this study are presented in Fig. S1. Initial expression tests showed that in our experimental conditions, NTT1 and misNTT1 were not expressed in Rosetta2 cells (Fig. 1) which is in opposition from what has recently been described [16]. For both NTT1 and misNTT1 expression was weak in BL21(DE3) and C41(DE3) (Fig. 1), but on the other hand, the expression level was high in C43(DE3) cells [22] with misNTT1 leading to quite higher protein amounts (Fig. 1). These results are consistent with two previously published concepts. Firstly, membrane proteins are usually well expressed in C43 cells, which is probably due to their ability to produce extra internal membranes [27]. Secondly, Mistic fusion has been proposed to pull membrane protein into the lipid bilayer independently of the Sec translocon. Therefore, misNTT1 expression into the membrane was greatly enhanced thanks to C43 cells and Mistic. Thus, overnight expression at 20 °C led to overall expression levels of about 2.5 mg- and 40 mg-/L of culture for NTT1 and misNTT1, respectively (Table 1). This 16 fold increase for misNTT1 expression level is promising, but its quality (folding and activity) has to be ascertained prior to structural studies.

3.1.2. Import and export of ATP

Transport measurements have been performed on whole *E. coli* cells, before solubilizing the membranes and purifying the proteins. Thus, the functional properties of the overexpressed proteins were assessed directly in the *E. coli* membrane prior to any modifications of their local environment. Transport activities have been measured by two independent methods: radioactive ATP uptake and cold ADP/ATP exchange followed by luminescence. The latter assay has been established in our team on the basis of previous experiments performed on purified mitochondria [28]. In this assay, addition of ADP induces a simultaneous and continuous ATP export from intact *E. coli* cells (Fig. 2A), which is monitored by the luminescence resulting from a luciferin/luciferase mix present in the external buffer (Fig. 2A). This method is complementary to radioactive ATP uptake measurements since it monitors the nucleotide transport in the opposite direction (export from *E. coli versus* import). Moreover, this assay also allows the monitoring of nucleotide exchange in real time and not just the determination of a net nucleotide import or export. This method is highly sensitive and specific as seen from the significant light emission obtained with NTT1 (Fig. 2A, NTT1 curve), in comparison to the flat curve obtained with bacteria containing an empty vector (Fig. 2A, ctl curve). The luminescence assay showed that the global release of ATP was very high and long-lasting in bacteria overexpressing NTT1 (Fig. 2A, NTT1 curve). On the contrary, cells overexpressing misNTT1 displayed an initial light increase smaller than for NTT1 expressing cells (Fig. 2A, first seconds after ADP addition)

Table 1
Comparison of the expression yield and activity of NTT1 and the different NTT1 mistic fusions. Expression yields of the different constructs have been determined by western-blot quantification. NTT1 relative activity corresponds to Fig. 2C. V_MK_M has been determined as described in the material and methods section.

Construct	Expression yield (mg/L of culture)	NTT1 relative activity (%)	$V_{M\text{-}ATP}$ (nmol ATP/min/mg NTT1)	$K_{M\text{-}ATP}$ (µM)	$K_{M\text{-}ADP}$ (µM)
NTT1	2.5	100	10.1 +/− 2.5	32 +/− 6.0	6.7 +/− 2.4
misNTT1	40	16.4	1.2 +/− 0.7	40.2 +/− 16.7	19.2 +/− 8.6
misTmNTT1	35	15.1	–	–	–
mislinkNTT1	0.06	6.6	–	–	–

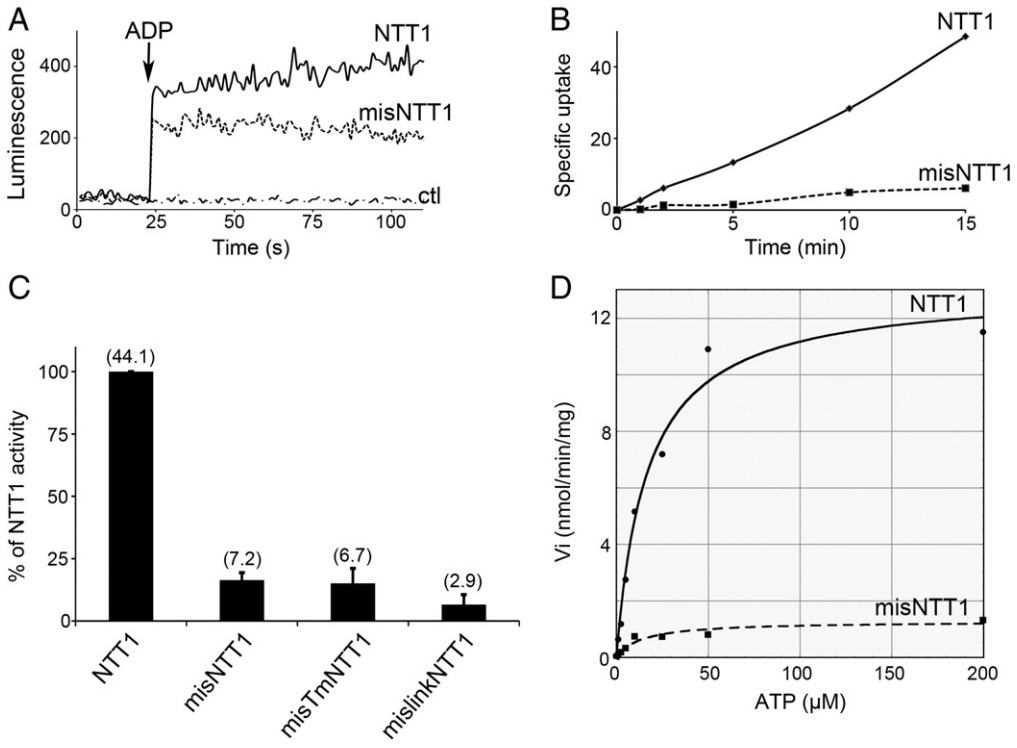

Fig. 2. Transport activity of NTT1 and misNTT1 fusions. Panel A, luminescence measurements for NTT1, misNTT1 expressing cells and background control (ctl) for an empty vector-containing cells. Panel B, specific radioactive ATP uptake kinetics for NTT1 and misNTT1 expressing cells in nmole of ATP per mg of NTT1 or misNTT1. Proteins were quantified by western-blot. These experiments have been performed using 50 μM ATP and for each curve the background uptake has first been subtracted. Panel C, 15 min time-point for NTT1, misNTT1, misTmNTT1 and mislinkNTT1 specific radioactive ATP uptake using 50 μM ATP comparison with NTT1 uptake defined as 100% level. Mean of three independent experiments. Amount of ATP imported per mg of NTT1 proteins is indicated into brackets. Panel D, NTT1 and misNTT1 V_MK_M experiments. Experimental points are shown with markers and fits shown with lines. For panels A, B and D one representative experiment is shown from a set of at least three independent experiments.

and then the emitted light tended to decrease. This effect is due to the fact that luciferase light emission is transient and depends on continuous supply of new ATP molecules. Thus misNTT1 exhibited a slower ADP/ATP transport activity than NTT1 (Fig. 2A).

In parallel, radioactive ATP uptake into *E. coli* cells overexpressing NTT1 or misNTT1 showed that the specific activity of misNTT1 was 5 to 10 times lower than that of NTT1 at 50 μM of ATP (Fig. 2B–C).

3.1.3. Transport rates

To compare in details the transport properties of NTT1 and misNTT1, V_M and K_M parameters were determined from radioactive ATP uptake assays. Regarding the high activity of NTT1 produced in *E. coli,* these velocity experiments were very robust and Michaelis–Menten equation fitted very well the experimental data (Fig. 2D and Table 1). On the contrary, the low transport activity of misNTT1 led to data with higher standard deviations (Fig. 2D and Table 1). NTT1 and misNTT1 K_M values for ATP were in the same range: 32 μM and 40 μM, respectively, but the misNTT1 V_M value was 10 times lower than that of NTT1 (Table 1). The K_M for ADP was determined through the luciferase assay in order to characterize the behavior with this nucleotide (Table 1). NTT1 and misNTT1 K_M values were 7 μM and 19 μM, respectively, in good agreement with a previously published value determined for NTT1 (12 μM) using radioactive ADP uptake measurements [29]. Therefore, while K_M values for ADP and ATP were in the same range, V_M values strongly differed for NTT1 and misNTT1.

3.2. Can the activity of misNTT1 be recovered?

3.2.1. The orientation of misNTT1 in the membrane is not responsible for its lower activity

One explanation for the lower activity of misNTT1, when compared to the one of NTT1, might result from an inverted integration of the Mistic fusion in *E. coli* membranes. A new Mistic fusion (termed misTmNTT1, see Fig. S1 and Table S1) has been constructed, containing one additional transmembrane α-helix at the C-terminus of Mistic in order to invert the orientation of the fused membrane protein across the bacterial membrane. Indeed, in misNTT1 the short linker between Mistic and NTT1 obligates the C-terminus of Mistic and the N-terminus of NTT1 to be on the same side of the membrane. Whether this orientation of NTT1 is appropriate for its function is not known. Although the N-terminus of NTT1 in misTmNTT1 should now be located at the opposite side of the membrane, the same low transport activity was observed (Fig. 2C and Table 1).

3.2.2. Mistic does not hinder the transport by conformational constraints

The lower activity of misNTT1 might also result from conformational constrains within the Mistic fusion. Indeed, a too short linker between Mistic and NTT1, could hinder conformational changes that are often necessary for transport mechanisms of molecules as large as nucleotides. To test such a hypothesis, a longer linker between Mistic and NTT1 (mislinkNTT1, Fig. S1 and Table S1) has been engineered in order to get rid of a potential locking effect due to the fusion. The linker has been enlarged from 10 to 25 residues and composed mainly of G, S, N and L in order to be rather hydrophilic and to increase its flexibility. However, the activity of mislinkNTT1 was similar to the ones of the other Mistic fusions tested (Fig. 2C and Table 1).

Furthermore, the expression yields of the different Mistic fusions were quite similar with the exception of mislinkNTT1, which was almost not expressed (Table 1). Thus, the low activity of those fusions is neither due to a saturation problem of any machinery, nor to an impairing of the dynamical properties of the membrane. Two points that could both result from a high level of membrane protein overexpression, which was not the case for mislinkNTT1.

3.2.3. Releasing NTT1 from misTevNTT1 increases its specific activity

In order to test whether the NTT1 moiety is correctly folded in the misNTT1 fusion, an *in vivo* fusion cleavage strategy was developed. For *in vivo* proteolysis of the fusion, a TEV cleavage site has been introduced into misNTT1 to generate misTevNTT1 (Fig. S1). The expression level and the activity of misTevNTT1 were similar to those of misNTT1 (not shown). A tetracycline-inducible plasmid, allowing the expression of a TEV protease active form *in vivo* has been constructed (Fig. 3A, Histag panel). In bacterial cells containing both plasmids Mistic was efficiently cleaved-off from misTevNTT1 located in the bacterial membrane by the TEV protease (Fig. 3A). Indeed, this co-expression led to the detection of both NTT1 mature form (*via Strep*tag detection, Fig. 3A, *Strep*tag panel) and Mistic alone (15 kDa, *via* Histag detection, Fig. 3A, Histag panel). Although this tetracycline-inducible expression system is tighter than others, promoter expression leaks have anyhow been observed, particularly in C43(DE3) cells. Therefore, BL21(DE3) cells have been selected as an alternative for these experiments. The transport activity has been followed by radioactive ATP uptake in cells expressing either TEV protease or misTevNTT1 only, as well as in cells co-expressing misTevNTT1 and TEV, either simultaneously or sequentially (first misTevNTT1, then TEV) (Fig. 3B). When compared to misTevNTT1 alone, the specific ATP uptake was increased three times when both misTevNTT1 and TEV were expressed simultaneously and four-fold when the two proteins were expressed sequentially. This last result clearly highlights the recovery of NTT1's activity after cleavage, once the Mistic fusion was already inserted into the membrane.

In conclusion about transport activities, all of the Mistic-NTT1 fusion proteins were considerably slowed down in comparison to NTT1's mature form. As evidenced by the transport measurements performed on four different constructs (NTT1, misNTT1, misTmNTT1, mislinkNTT1, Fig. S1), the decrease in transport activity results neither from an inverted orientation of NTT1 across the membrane, nor to a problem of locked conformation due to steric hindrance. Improper folding of NTT1 in the Mistic fusions can also be ruled out from our experiments. Indeed, in *E. coli* membranes, misNTT1 retains native binding sites for ADP and ATP as evidenced by K_M determination and the cleaved fusion recovers the activity of mature NTT1. Based on these observations, folding and quaternary structures were further characterized to get a better molecular understanding of NTT1/misNTT1 differences.

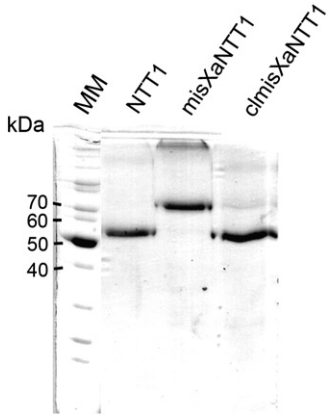

Fig. 4. NTT1, misXaNTT1 and cleaved misXaNTT1 purification. Assessment of the final purity of NTT1, misXaNTT1 and clmisXaNTT1 on Coomassie-stained 10% acrylamide SDS-PAGE. 5 μg of each protein have been loaded. MM corresponds to the molecular weight marker lanes.

3.3. Analysis of overall-fold and quaternary structures of recombinant NTT1, misNTT1 and cleaved Mistic NTT1 (clmisXaNTT1)

3.3.1. Purification of NTT1, misNTT1 and clmisXaNTT1

In order to perform an in-depth molecular characterization of the three proteins, NTT1, misXaNTT1 and the cleaved fusion clmisXaNTT1 have to be obtained in solution and homogeneous before biochemical/biophysical analysis. misXaNTT1 and clmisXaNTT1 were purified using the same overall approach as the one developed for NTT1: LAPAO solubilization followed by Immobilized Metal Ion Affinity Chromatography (IMAC) and *Strep*-Tactin chromatography steps. For the production of clmisXaNTT1, several misNTT1 constructs have been designed to enable the cleavage of the fusion and the subsequent purification of NTT1 mature form after Mistic removal. For that purpose, several specific protease cleavage sites have been introduced and tested. Factor Xa cleavage site provided the best cleavage yields and was therefore chosen for subsequent studies. This fusion, called misXaNTT1, kept the same properties (production level and activity in *E. coli)* as misNTT1 (not shown). The three NTT1 forms have all been obtained with a very similar and satisfying final purity (Fig. 4) with

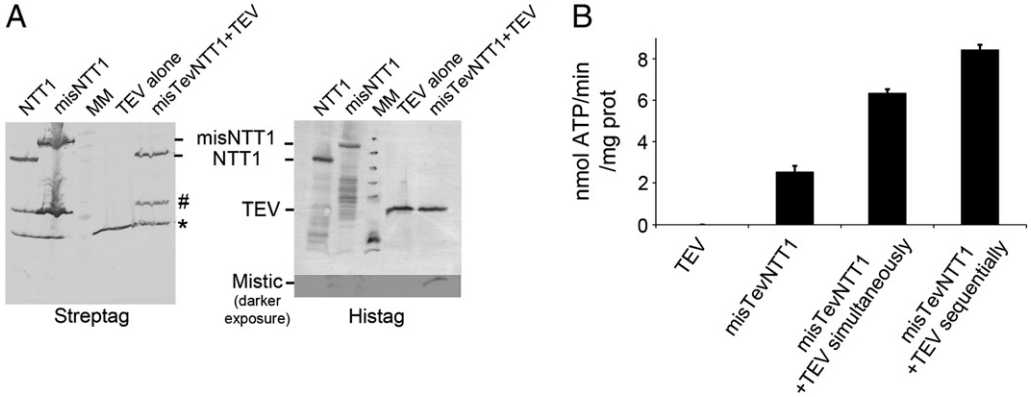

Fig. 3. Production and specific radioactive ATP uptake of *in vivo* cleaved misTevNTT1. Panel A, Detection *via* Histag (right panel), *Strep*tag (left panel) of both NTT1 or misNTT1 expressed in C43(DE3) and TEV and misTevNTT1 proteolysis products expressed in BL21(DE3). Due to its small size and low abundance Mistic required a longer exposure to be detected as indicated on the figure. * indicates the BCCP, an endogenously biotinylated protein always detected by *Strep*-Tactin peroxidase in whole bacterial extracts and # probably corresponds to a NTT1 by-product generated during expression. 2 mg of whole cells have been loaded per lane. MM corresponds to the molecular weight marker lanes. Panel B, specific activity for TEV alone, misTevNTT1 alone and misTevNTT1 and TEV expressed simultaneously or sequentially using 50 μM ATP. Activities are expressed in nmole of ATP/min/mg of transporter. For TEV, no quantity of protein was taken into consideration.

yields of about 0.5 mg, 3 mg and 2 mg for NTT1, misXaNTT1 and clmisXaNTT1, respectively, from 1 L of culture.

3.3.2. NTT1 is most probably correctly folded within misXaNTT1

The solubilization patterns of NTT1 and misXaNTT1 from *E. coli* membrane using detergents having different physico-chemical properties gave first indications of similarities or differences in the overall fold of the two proteins. Several detergents were tested: octaethylene glycol monododecyl ether ($C_{12}E_8$), β-dodecylmaltoside (DDM), β-octylglucoside (OG), laurylamidodimethylpropylaminoxyde (LAPAO), lauryldimethylaminoxyde (LDAO) and Fos-choline12 (FC12). For both NTT1 and misXaNTT1, $C_{12}E_8$, DDM and OG were not or poorly efficient to solubilize any protein (Fig. 5A–B), while NTT1 and misXaNTT1 were well solubilized from membranes by LDAO and even more efficiently by LAPAO and FC12 (Fig. 5A–B). However, NTT1 and misXaNTT1 were not solubilized to the same extent: while the former was almost 100% solubilized by LAPAO, for misXaNTT1 only 30–40% of the protein can be solubilized by this detergent (Fig. 5A–B). This limited solubilization of misXaNTT1 was the main reason to explain the limited yield of purified misXaNTT1 and clmisXaNTT1 regarding the expression yield of misXaNTT1.

The three proteins NTT1, misNTT1 and clmisXaNTT1 purified in LAPAO were also assessed by limited proteolysis to highlight putative compact domains [25]. Herein, misNTT1 was used instead of misXaNTT1 to avoid a preferred limited proteolysis site at the factor Xa cleavage sequence. Several proteases were used: chymotrypsin (Fig. 5C–E), trypsin and elastase (not shown), but all three gave similar results. NTT1 and clmisXaNTT1 (both indicated with *) had a very similar behavior (Fig. 5C and E) and limited proteolysis led to a single fragment corresponding to clmisXaNTT1. Indeed, during proteolysis, NTT1 lost its five N-terminal residues to reach the size of the clmisXaNTT1. misNTT1 (indicated with #) was proteolysed into two stable fragments which sizes correspond to Mistic (indicated with §) and NTT1 (Fig. 5D). The two fragments of misNTT1 were already visible after 15 min and misNTT1 was completely cleaved within 120 min. Thus, misNTT1 seems to encompass two compact and independently structured domains: Mistic and NTT1, demonstrating that NTT1 is most probably well folded within the fusion protein.

3.3.3. Oligomeric state of NTT1 is recovered following cleavage of misXaNTT1

Oligomerization might be an important issue for the activity. Therefore, the oligomeric states of NTT1, misXaNTT1 and clmisXaNTT1 have been assessed by SEC and analytical ultracentrifugation (AUC). SEC elution profiles of NTT1 and clmisXaNTT1 were quite similar and revealed two main species in the intermediate molecular mass range, as well as the presence of a few other higher molecular mass species (Fig. 6A). In contrast, misXaNTT1 had a completely different oligomeric behavior: the protein eluted as quite a broad peak of higher molecular mass than that of NTT1 and clmisXaNTT1

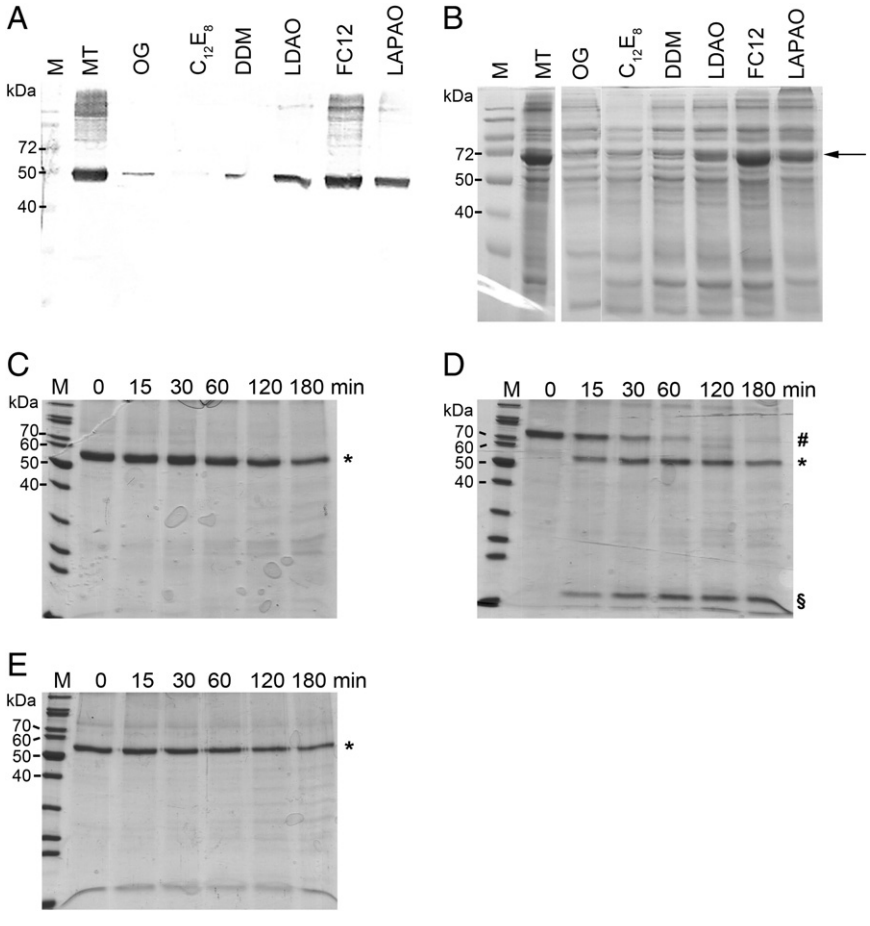

Fig. 5. Overall fold of NTT1, misNTT1 and clmisXaNTT1. Panel A, NTT1 from overexpressing membranes extracted by different detergents. Solubilized NTT1 was detected by *Strep*-Tactin peroxidase western-blot. 10 μg of total membrane proteins have been loaded into each lane. Panel B, misXaNTT1 from overexpressing membranes extracted by different detergents. Solubilized Mistic fusion was detected as a band at 70 kDa on Coomassie-stained SDS-PAGE, shown with the arrow. 10 μg of total membrane proteins have been loaded into each lane. Panels C, D and E, kinetic of NTT1 (C), misNTT1 (D) and clmisXaNTT1 (E) chymotrypsinolysis between 0 and 180 min. NTT1 is indicated with *, misNTT1 with # and Mistic alone with §. 5 μg of total proteolyzed protein have been loaded into each lane. M corresponds to the molecular weight marker lanes and MT corresponds to the total membrane protein control.

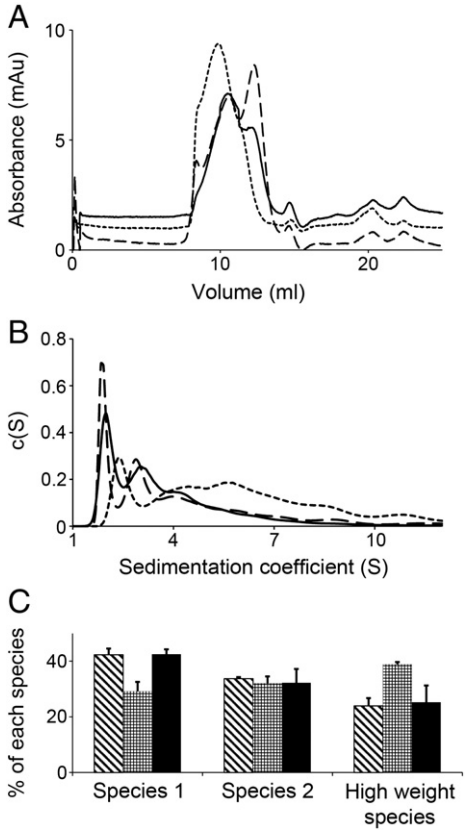

Fig. 6. NTT1, misXaNTT1 and clmisXaNTT1 quaternary organizations. Panel A, pure NTT1 (long dash line), misXaNTT1 (small dash line) and clmisXaNTT1 (continuous line) size exclusion chromatography. Panel B, pure NTT1 (long dash line), misXaNTT1 (small dash line) and clmisXaNTT1 (continuous line) sedimentation coefficient distributions from sedimentation velocity experiments. Panel C, NTT1 (hashed bar), misXaNTT1 (squared bar) and clmisXaNTT1 (black bar) AUC species distribution analysis over three independent experiments.

(Fig. 6A). This difference cannot result from the mass increase induced by the fusion to Mistic (13 kDa). To assess the quaternary structure of misXaNTT1 more precisely, AUC sedimentation velocity experiments have been performed. NTT1 was mainly present as a 1.9 S (species 1) and a 2.9 S (species 2) species (Fig. 6B), and clmisXaNTT1 shows a similar species distribution (Fig. 6B). misXaNTT1 had a more heterogeneous oligomeric content with mainly high molecular mass species centered around 5.5 S (Fig. 6B). The results for the three proteins were highly reproducible over different purified protein batches. The relative proportions of species 1, species 2 and high molecular weight species have been averaged over three independent purifications and showed that large oligomers were twice more present in misXaNTT1 than in NTT1 or clmisXaNTT1 (Fig. 6C). Interestingly, our results showed that misXaNTT1 after cleavage into clmisXaNTT1 returns to an oligomerization status identical to NTT1.

4. Conclusions

The determination of the high-resolution structure of eukaryotic membrane transporters is hampered by difficulties in obtaining protein crystals. As such, the availability of pure recombinant proteins in relative abundance allows wide screening of crystallization conditions and increases the likelihood of getting diffracting crystals. Herein, we demonstrated that fusion with Mistic results in increased level of recombinant ATP/ADP transporter production. While, the fusion protein has a strongly affected transport activity in *E. coli* membranes, *in vivo* fusion cleavage led to the delivery of a functional transporter. Furthermore, molecular characterization clearly showed that NTT1 forms an independent and well-folded transporter within the Mistic fusion. Moreover, we have shown that the amount of purified clmisXaNTT1 is four times higher than the quantity obtained from the purification of NTT1 produced as a mature protein. This production yield could be further increased by fine-tuning the expression level and/or by co-expressing chaperones to increase the amount of well-folded protein. Even though the use of Mistic has been successfully reported since its initial description in the literature [8] its mechanism of action is still not understood. However, it seems that Mistic has the ability to pull membrane proteins into *E. coli* membrane most probably *via* Mistic oligomers. Indeed, we showed that oligomeric status equilibrium turns to large oligomers formed by Mistic boundaries in misNTT1 fusion. Furthermore, the ten times transport rate decrease in misNTT1 in comparison to NTT1 mainly relates from this oligomeric status alteration. Indeed, Mistic multimers could interfere with a proper NTT1 interface. It is therefore important to keep in mind this Mistic polymerization effect, when using the Mistic fusion strategy. Finally, in the case of NTT1 the low specific activity of misNTT1 might also contribute to its strong overexpression by reducing potential detrimental effect on E. coli metabolism.

In conclusion, we explored expression, purification, activity and biochemical/biophysical properties of a chloroplast ATP/ADP transporter fused to Mistic. The low specific activity of the Mistic-transporter fusion did not circumvent the interest of this approach for large scale purification of membrane proteins. Indeed, NTT1 is properly folded and can be delivered in a native state after fusion cleavage.

Supplementary materials related to this article can be found online at doi:10.1016/j.bbamem.2011.04.011.

Acknowledgments

We are grateful to Christine Ebel and Aline Le Roy for access to analytical ultracentrifuge and for helpful discussions and advices. We acknowledge Jean-Michel Jault for access to fluorimeter. We thank Corinne Vivès for critically reading the manuscript. This work was supported by the CEA (CEA-PM program), the CNRS (post-doctoral fellowship to AFB), the Université Joseph Fourier Grenoble 1, The Institut Universitaire de France, the EU specific targeted research project IMPS and the Association Française contre les Myopathies (post-doctoral fellowship to AD).

References

[1] J. Liu, B. Rost, Comparing function and structure between entire proteomes, Protein Sci. 10 (2001) 1970–1979.
[2] S. White, http://blanco.biomol.uci.edu/Membrane_Proteins_xtal.html (website).
[3] V. Cherezov, D.M. Rosenbaum, M.A. Hanson, S.G. Rasmussen, F.S. Thian, T.S. Kobilka, H.J. Choi, P. Kuhn, W.I. Weis, B.K. Kobilka, R.C. Stevens, High-resolution crystal structure of an engineered human beta2-adrenergic G protein-coupled receptor, Science 318 (2007) 1258–1265.
[4] E. Pebay-Peyroula, G. Rummel, J.P. Rosenbusch, E.M. Landau, X-ray structure of bacteriorhodopsin at 2.5 angstroms from microcrystals grown in lipidic cubic phases, Science 277 (1997) 1676–1681.
[5] E.M. Landau, J.P. Rosenbusch, Lipidic cubic phases: a novel concept for the crystallization of membrane proteins, Proc. Natl. Acad. Sci. U. S. A. 93 (1996) 14532–14535.
[6] K. Lundstrom, Structural genomics for membrane proteins, Cell. Mol. Life Sci. 63 (2006) 2597–2607.
[7] M.A. Hanson, A. Brooun, K.A. Baker, V.P. Jaakola, C. Roth, E.Y. Chien, A. Alexandrov, J. Velasquez, L. Davis, M. Griffith, K. Moy, B.K. Ganser-Pornillos, Y. Hua, P. Kuhn, S. Ellis, M. Yeager, R.C. Stevens, Profiling of membrane protein variants in a baculovirus system by coupling cell-surface detection with small-scale parallel expression, Protein Expr. Purif. 56 (2007) 85–92.
[8] T.P. Roosild, J. Greenwald, M. Vega, S. Castronovo, R. Riek, S. Choe, NMR structure of Mistic, a membrane-integrating protein for membrane protein expression, Science 307 (2005) 1317–1321.
[9] G. Kefala, W. Kwiatkowski, L. Esquivies, I. Maslennikov, S. Choe, Application of Mistic to improving the expression and membrane integration of histidine kinase receptors from *Escherichia coli*, J. Struct. Funct. Genomics 8 (2007) 167–172.
[10] O.V. Nekrasova, A.N. Wulfson, R.V. Tikhonov, S.A. Yakimov, T.N. Simonova, A.I. Tagvey, D.A. Dolgikh, M.A. Ostrovsky, M.P. Kirpichnikov, A new hybrid protein for production of recombinant bacteriorhodopsin in *Escherichia coli*, J. Biotechnol. 147 (2010) 145–150.

[11] L.E. Petrovskaya, A.A. Shulga, O.V. Bocharova, Y.S. Ermolyuk, E.A. Kryukova, V.V. Chupin, M.J. Blommers, A.S. Arseniev, M.P. Kirpichnikov, Expression of G-protein coupled receptors in *Escherichia coli* for structural studies, Biochemistry (Mosc) 75 (2010) 881–891.
[12] H. Dvir, S. Choe, Bacterial expression of a eukaryotic membrane protein in fusion to various Mistic orthologs, Protein Expr. Purif. 68 (2009) 28–33.
[13] K.Y. Blain, W. Kwiatkowski, S. Choe, The functionally active mistic-fused histidine kinase receptor, EnvZ, Biochemistry 49 (2010) 9089–9095.
[14] H.E. Neuhaus, E. Thom, T. Möhlmann, M. Steup, K. Kampfenkel, Characterization of a novel eukaryotic ATP/ADP translocator located in the plastid envelope of *Arabidopsis thaliana*, Plant J. 11 (1997) 73–82.
[15] T. Möhlmann, J. Tjaden, C. Schwöppe, H.H. Winkler, K. Kampfenkel, H.E. Neuhaus, Occurrence of two plastidic ATP/ADP transporters in Arabidopsis thaliana L.—molecular characterisation and comparative structural analysis of similar ATP/ADP translocators from plastids and Rickettsia prowazekii, Eur. J. Biochem. 252 (1998) 353–359.
[16] O. Trentmann, B. Jung, H.E. Neuhaus, I. Haferkamp, Nonmitochondrial ATP/ADP transporters accept phosphate as third substrate, J. Biol. Chem. 283 (2008) 36486–36493.
[17] O. Trentmann, C. Decker, H.H. Winkler, H.E. Neuhaus, Charged amino-acid residues in transmembrane domains of the plastidic ATP/ADP transporter from *arabidopsis* are important for transport efficiency, substrate specificity, and counter exchange properties, Eur. J. Biochem. 267 (2000) 4098–4105.
[18] O. Trentmann, M. Horn, A.C. Terwisscha van Scheltinga, H.E. Neuhaus, I. Haferkamp, Enlightening energy parasitism by analysis of an ATP/ADP transporter from *chlamydiae*, PLoS Biol. 5 (2007) e231.
[19] A. Frelet-Barrand, S. Boutigny, L. Moyet, A. Deniaud, D. Seigneurin-Berny, D. Salvi, F. Bernaudat, P. Richaud, E. Pebay-Peyroula, J. Joyard, N. Rolland, *Lactococcus lactis*, an alternative system for functional expression of peripheral and intrinsic *Arabidopsis* membrane proteins, PLoS One 5 (2010) e8746.
[20] F. van den Ent, J. Lowe, RF cloning: a restriction-free method for inserting target genes into plasmids, J. Biochem. Biophys. Methods 67 (2006) 67–74.
[21] K. Nishihara, M. Kanemori, M. Kitagawa, H. Yanagi, T. Yura, Chaperone coexpression plasmids: differential and synergistic roles of DnaK-DnaJ-GrpE and GroEL-GroES in assisting folding of an allergen of Japanese cedar pollen, Cryj2, in Escherichia coli, Appl. Environ. Microbiol. 64 (1998) 1694–1699.
[22] B. Miroux, J.E. Walker, Over-production of proteins in *Escherichia coli*: mutant hosts that allow synthesis of some membrane proteins and globular proteins at high levels, J. Mol. Biol. 260 (1996) 289–298.
[23] E.M. Krammer, S. Ravaud, F. Dehez, A. Frelet-Barrand, E. Pebay-Peyroula, C. Chipot, High-chloride concentrations abolish the binding of adenine nucleotides in the mitochondrial ADP/ATP carrier family, Biophys. J. 97 (2009) L25–L27.
[24] S. Thuswaldner, J.O. Lagerstedt, M. Rojas-Stutz, K. Bouhidel, C. Der, N. Leborgne-Castel, A. Mishra, F. Marty, B. Schoefs, I. Adamska, B.L. Persson, C. Spetea, Identification, expression, and functional analyses of a thylakoid ATP/ADP carrier from *Arabidopsis*, J. Biol. Chem. 282 (2007) 8848–8859.
[25] A. Deniaud, A. Goulielmakis, J. Covès, E. Pebay-Peyroula, Differences between CusA and AcrB crystallisation highlighted by protein flexibility, PLoS One 4 (2009) e6214.
[26] P. Schuck, P. Rossmanith, Determination of the sedimentation coefficient distribution by least-squares boundary modeling, Biopolymers 54 (2000) 328–341.
[27] I. Arechaga, B. Miroux, S. Karrasch, R. Huijbregts, B. de Kruijff, M.J. Runswick, J.E. Walker, Characterisation of new intracellular membranes in *Escherichia coli* accompanying large scale over-production of the b subunit of F(1)F(o) ATP synthase, FEBS Lett. 482 (2000) 215–219.
[28] G. Brandolin, A. Le Saux, V. Trézéguet, P.V. Vignais, G.J. Lauquin, Biochemical characterisation of the isolated Anc2 adenine nucleotide carrier from *Saccharomyces cerevisiae* mitochondria, Biochem. Biophys. Res. Commun. 192 (1993) 143–150.
[29] J. Tjaden, C. Schwöppe, T. Möhlmann, P.W. Quick, H.E. Neuhaus, Expression of a plastidic ATP/ADP transporter gene in *Escherichia coli* leads to a functional adenine nucleotide transport system in the bacterial cytoplasmic membrane, J. Biol. Chem. 273 (1998) 9630–9636.